(125) EXPERIMENTAL STUDY ON STRUCTURAL FAILURE OF STEEL ANGLE MEMBERS DUE TO VERY LOW CYCLE FATIGUE UNDER EARTHQUAKE LOADING

Graduate Student, Kyoto University, Yeon-Soo PARK
Research Associate, Disas. Prev. Res. Inst., Kyoto University, Satoshi IWAI
Professor, Disas. Prev. Res. Inst., Kyoto University, Taijiro NONAKA
Professor, Disas. Prev. Res. Inst., Kyoto University, Hiroyuki KAMEDA

Abstract An experimental investigation is made of very low cycle fatigue of steel angle specimens under large repeated deformations. The objective is to extract decisive factors causing cracks and ultimate failure in the course of loading repetitions of the order of a few to twenty cycles. The angle specimen was subjected to repeated axial load after undergoing inelastic buckling. The experimental investigation shows that the initiation of cracking due to very low cycle fatigue is closely related to cumulative local strains of the order of 25-40%, regardless of loading patterns, deflection modes, and width-to-thickness ratios.

Introduction Well-designed steel structures may be expected to undergo partial plastic deformation under strong seismic excitations; structural damage and failure are often associated with plastic and unstable behavior of structural members due to large cyclic deformations with initiation of local buckling. Therefore, it is important to identify the decisive factors causing very low cycle fatigue, which is herein meant to be structural fatigue under loading repetitions of the order of a few to twenty cycles. Previous experimental research on very low cycle fatigue involved thin-plate elements in a steel member.[1] The research result showed that the state of ultimate failure under cyclic loading is strongly related to the maximum strain taking place at an edge or corner in the cross-section. The studies described in this paper are focused on observing the inelastic post-buckling behavior of steel members in order to clarify the quantitative relationships among the important physical factors of cumulative plastic failure. Particular attention is paid to the effects of loading conditions and cross-sectional shapes on very low cycle fatigue behavior.

Specimens and Testing Parameters The test specimens were angles L-40x40x3 and L-40x40x5 of SS41 grade. The yield stress and the ultimate tensile strength of the materials were ranged 339-344 N/mm^2 and 456-470 N/mm^2, respectively. The average elongation in the material test varied between 27%-33%. A steel plate of 9mm thickness was attached by welds perpendicularly at each end of the specimen, as indicated in Fig. 1. Testing parameters are summarized as follows: (1)Width-to-thickness ratios b/t; (2)loading patterns; and (3)deflection modes. The value of (1) was selected 15.8-16.4 and 8.6, as shown in Table 1. The choices of (2) were increased displacement amplitude loading(I type) or constant displacement amplitude loading(C type) in the compression side, as shown in Fig. 2. The definition of (3) is described on the next page. Each specimen was pin-supported at both ends with the length L of the tested part between pin-supports being 300-318mm, as shown in Table 1 and Fig. 3. The slenderness ratios of the specimens ranged 37-41.

Loading and Measurement Systems The experiments were performed up to the occurrence of visible cracks or rupture of the specimen, in order to observe the deteriorating process and the state of cumulative strains at the critical part of the specimen. A slowly varying uni-axial load was applied to the centroid G of the cross-section of each specimen[Fig. 1(d)], using a hydraulic servo actuator with a loading capacity of 294kN. The load was controlled by the relative axial displacement Δ, programmed as in Table 1, between both ends approaching each other. This causes buckling in the specimen under first compression loading, and induces very high strains. In order to measure residual local edge strains after testing, dots on the surface were marked at

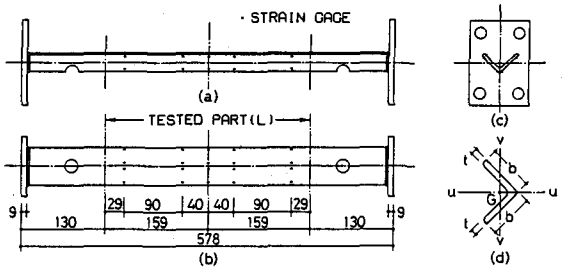

Fig. 1 Test specimen(length in mm)

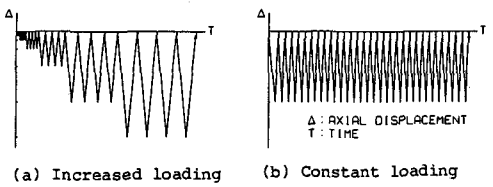

Fig. 2 Loading patterns

Table 1 Loading parameters and results

Specimen Name	No.	L(mm)	b(mm)	t(mm)	b/t	(Δ/L)x100	Mode of Deflection	P_{cr}(kN)	Extreme Strain tens.	comp.
L3IN	4	301	40.4	2.55	15.8	-0.5 - 0 (4) -1.0 - 0 (4) -2.0 - 0 (4) -4.0 - 0 (3) -8.0 - 0 (4) -12.0 - 0 (4)	N	58.02	-	-
L3CP	6	300	40.3	2.55	15.8	-8.0 - 0(16)	P	62.92	27.5%	-29%
L3CN	5	301	40.5	2.47	16.4	-8.0 - 0(30)	N	68.31	25%	-41%
L5IP	9	318	39.2	4.56	8.6	-0.5 - 0 (4) -0.9 - 0 (4) -1.9 - 0 (4) -3.8 - 0 (4) -7.6 - 0 (4) -11.3 - 0 (4)	P	100.65	35%	-35%
L5IN	7	300	39.2	4.58	8.6	-0.6 - 0 (4) -1.0 - 0 (4) -2.0 - 0 (2) -4.0 - 0 (4) -8.0 - 0 (4) -12.0 - 0 (4)	N	119.07	25%	-30%
L5CPa	8	317	39.3	4.55	8.6	-7.6 - 0(19)	P	95.55	32.5%	-35%
L5CPb	10	317	39.2	4.55	8.8	-7.6 - 0(19)	P	108.33	30%	-32.5%

[Note] I : Increasing amplitude, C : Constant amplitude
P : Positive deflection, N : Negative deflection
b : Width of angle leg, t : Thickness of angle leg
Δ : Relative axial displacement, ( ) : No. of cycles
L : Specimen length between pin-supports
P_{cr} : Buckling load

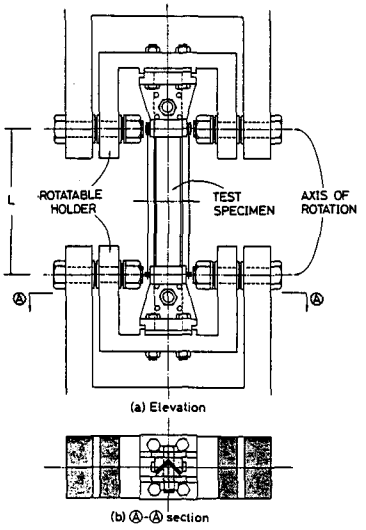

Fig. 3 Specimen supporting system

a 2mm pitch parallel to the longitudinal axis for a mid-part length of 80mm, using a Vickers hardness tester.

Buckling and Cracking Behavior Fig. 4 is a sketch of the buckling deformation and the states of visible cracking. The positive(P type) and negative(N type) deflection modes were observed as defined in the figure. The global buckling deformation was accompanied by local deformation(buckling of plate elements, i.e., of legs) at the mid-part of specimen. Irrespective of the deflection modes, visible cracks were initiated on the concave side of the overall buckling deformation when the specimen was stretching. Visible cracks at the convex side were observed within 1-3 cycles following the concave side cracking. Cracking at the concave and convex sides rapidly penetrated through the thickness of the legs. The cracks were quickly enlarged in the course of load repetitions. The cases of L5CPa and L5CPb specimen were loaded until the complete failure was attained.

Load-Deformation Relations Typical load-axial displacement relations of the specimens are shown in Fig. 5. Here the load P and relative displacement Δ are normalized by the yield load N_y and the length L, respectively. In most specimens subjected to increased amplitude loading, no cracks were observed under the repetition of global strain Δ/L smaller than or equal to 8%, but visible cracks were

initiated in the 1st cycle at the amplitude level of 12% global strain. In the cases of constant amplitude loading under 8% global strain, visible cracks occurred during the 7-9th cycle. The specimens of L5CPa and L5CPb under the same loading condition were completely broken in the identical 19th cycle with very similar load-displacement curves, as observed in (b) and (d) of Fig. 5. This is an indication of the trustworthiness of this series of fatigue tests. Fig. 6(a) and (b) show the relations between the load and lateral deflection corresponding to the load-displacement curves in Fig. 5(a) and (b), respectively. Inelastic buckling caused a sudden decrease in the compressive load-carrying capacity, but only a slight decrease in the tensile load-carrying capacity. However, both the compressive and tensile load-carrying capacities were considerably decreased by the initiation of cracking. It is thus found that the ultimate stage of failure is closely related to the occurrence of a visible crack.

Energy Dissipation Behavior The dissipated energy was calculated by the summation of the areas surrounded by the load-axial displacement curves. The relationships between the dissipated energy E and the number of cycles f are shown in Fig. 7 for all the specimens, where E_o is the maximum elastic strain energy which can be stored

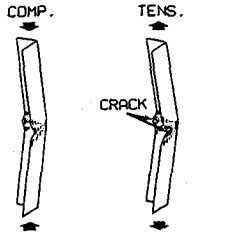

(a) Positive mode(L5IP)

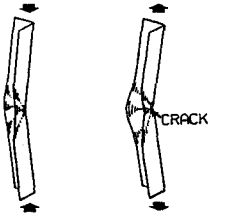

(b) Negative mode(L5IN)

Fig. 4 Deflection modes and cracking patterns

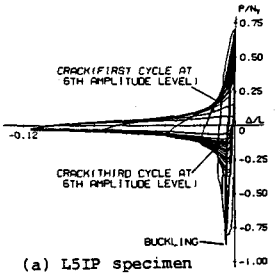

(a) L5IP specimen

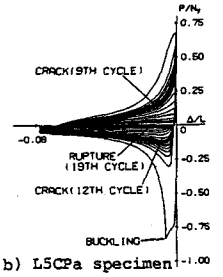

(b) L5CPa specimen

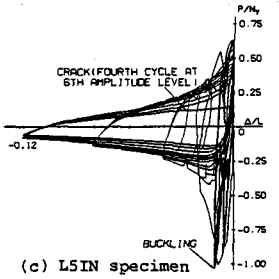

(c) L5IN specimen

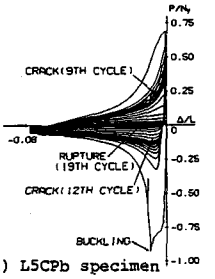

(d) L5CPb specimen

Fig. 5 Load-axial displacement relations

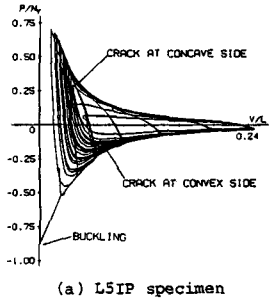

(a) L5IP specimen

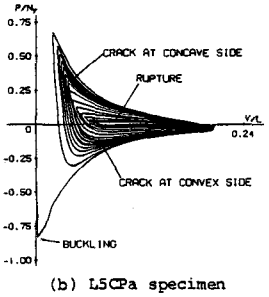

(b) L5CPa specimen

Fig. 6 Load-deflection relations

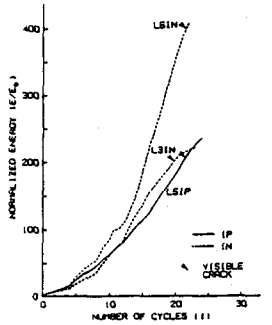

(a) Increased loading

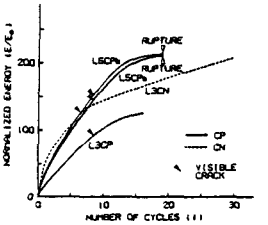

(b) Constant loading

Fig. 7 Comparison of cumulative energy dissipation in the course of increasing No. of cycles

in the tested part of the specimen. In the cases of the same loading pattern and the same deflection mode, very similar processes of energy absorption were observed [see curves for L5CPa and L5CPb in Fig. 7(b)]. If the deflection modes are different, however, the cumulative energy absorption processes were clearly different even among the specimens under the same loading pattern. No simple quantitative relations were observed between the initiation of a visible crack and the energy absorption capacity. Energy absorption processes and capacities depend upon the entire history of loading and the failure mode.

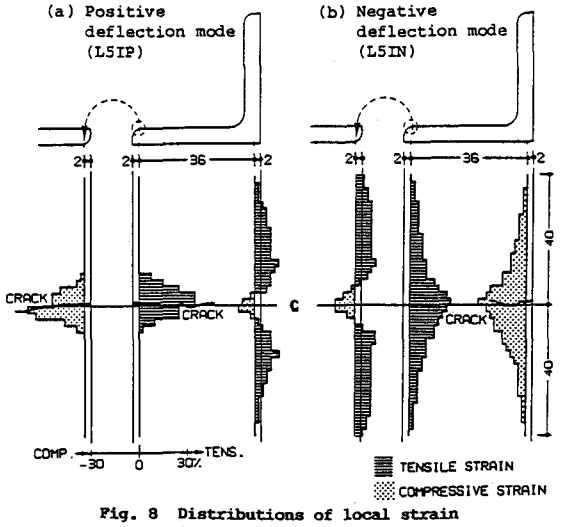

Fig. 8 Distributions of local strain in angle test

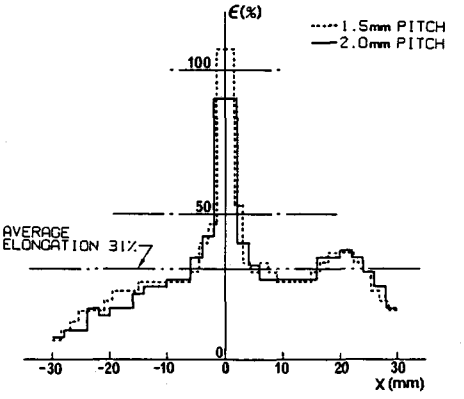

Fig. 9 Distribution of local strain in material test

Local Strain Distributions Fig. 8 shows typical distributions of residual local strains accumulated at the edges of legs after testing. Visible cracks are located near the regions of a severe concentration of strains. The maximum values of cumulative "net" strains, excluding contributions from the crack opening, of all the specimens were in the range of 25-35% on the elongation side and 30-40% on the contraction side (see Table 1), and they do not depend upon the loading patterns, the failure modes, and the width-to-thickness ratios. For comparison, Fig. 9 shows the local strain distributions in the monotonic tensile test of a JIS specimen of 13-B type. The maximum net strain in this material test was about 100%, even though the average elongation was about 30%. The cumulative strain values reflect the effects of the cyclic loading.

Conclusions The main conclusions from this investigation are summarized as follows:

1) The experimental investigation reveals that, regardless of loading patterns and deflection modes, visible cracks were initiated during stretching on the concave side of the overall bending deformation induced in the preceding load cycles.

2) The reappearance of very low cycle fatigue behavior was observed under the identical loading pattern and deflection mode, indicating the reliability of the experimental investigation.

3) The energy absorption capacity varies heavily with the history of loading and the failure mode.

4) The cumulative strains at the initiation of a visible crack due to the very low cycle fatigue were of the order of 25-40%, regardless of the loading patterns, the deflection modes, and the width-to-thickness ratios.

Reference 1) S. Iwai, T. Nonaka, U. Bourgund and H. Kameda: Structural Failure due to Very Low Cycle Fatigue of Steel Members and Elements under Earthquake Loading, Proc. of 8th Japan Earthquake Engrg. Symp., Vol. 2, 1990, pp. 1377-1382.